Novel Lead-Walled Straw PET Detector for Specialized Imaging Applications

Nader N. Shehad, M.E.E., Athanasios Athanasiades, Christopher S. Martin, Liang Sun, and Jeffrey L. Lacy, Ph.D.

***Abstract*— This project pursues development of PET cameras for specialized imaging applications such as small animal and breast imaging through a novel approach using low-cost, lead walled straw (LWS) modules. A 50 cm × 4.4 cm × 1.9 cm LWS module has been developed which operates at high singles rates, achieves 3.3 mm longitudinal resolution, and implements full 3D position decoding with inexpensive efficient electronics. The long linear module geometry together with full 3D position decoding affords use of a novel PET detector geometry consisting of two closely spaced long modules essentially in contact with the imaged object. This unique geometry provides efficiency through coverage of a very large solid angle and also a very large longitudinal field of view using a small number of coincidence modules.**

***Index Terms*— PET, breast imaging, small animal imaging, straw detectors.**

I. Introduction & Background

An extraordinary emphasis is currently being placed on the design and use of PET cameras for small animal studies, breast imaging, and other small-region specialized applications where sensitivity can be markedly enhanced by compressed geometry. Depth of interaction error in the 1 cm or greater crystal depth required in contemporary devices causes severe degradation of off-axis resolution in the specialized compressed geometry application. This project pursues development of PET cameras for such applications through the novel approach of using low cost, easily fabricated, lead walled straw (LWS) detectors. In a Phase II NIH project, feasibility of application of this high energy physics spin-off technology has been demonstrated. A 50 cm × 4.4 cm × 1.9 cm 50 straw module has been developed which operates at high singles rates, and achieves full 3D position decoding with inexpensive electronics. We explore application of such detector modules operated in coincidence pairs with close spatial separation. This unique geometry affords very large angular sampling (see Figure 1) and lengthy longitudinal field of view and thus high efficiency over exceptionally large imaging fields. This capability is made possible by the full 3D position encoding afforded by the wire detectors which provide for each event not only straw identity but also longitudinal position through resistive anode wire charge division.

Because an accurate 3D position can be determined for each gamma interaction, image resolution is not sacrificed even for very close detector spacing. In a breast imaging application the patient would be imaged in the prone position, with breast suspended through an opening in the bed with two detector module arrays positioned parallel to one another, and on either side of the breast. Detectors can be rotated together around a vertical axis $\pm 90^o$ during image acquisition if desired or remain static taking advantage of the wide static angular acceptance. The second important application under consideration for such PET camera design is small animal imaging. In this application a long linear closely spaced detector pair is rotated about its long central axis. With this design high sensitivity and very large axial field of view are achieved with a minimal number of detectors and thus markedly lower cost than is possible with crystal systems. Figure 2 shows results of a simulation comparing the sensitivity of a straw camera to that of a typical crystal camera. The hypothetical straw system consisted of two rectangular detector panels separated by 6 cm, each of dimensions 50 × 12 × 5.2 cm^3, containing nine 50-straw modules. The crystal-based camera consisted of two panels separated by 11 cm, each of dimensions 9.88 × 9.88 × 1 cm^3, and containing approximately 1000 3.1 × 3.1 × 10 mm^3 GSO crystals. A 350 keV energy cut was applied, and multiple crystal detections were discarded. Must add brief summary of comparison the point is we get better sensitivity over a reasonable breast field of view with minimal number of modules.

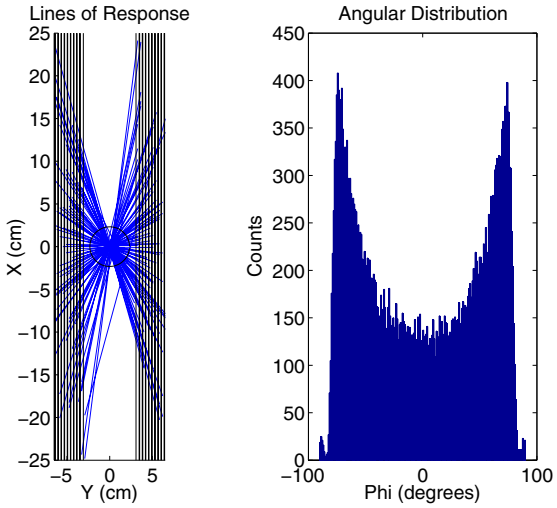

Fig. 1. Monte Carlo simulation for camera composed of two 50 cm × 4.4 cm × 1.9 cm LWS modules 6 cm apart showing the large angular acceptance.

Authors are with Proportional Technologies, Inc. 8022 El Rio St., Houston, TX 77054, Tel: 713-747-7324, E-mail: nshehad@proportionaltech.com. This work was supported by the NIH under SBIR Grant #s: RR13482 and RR15993.

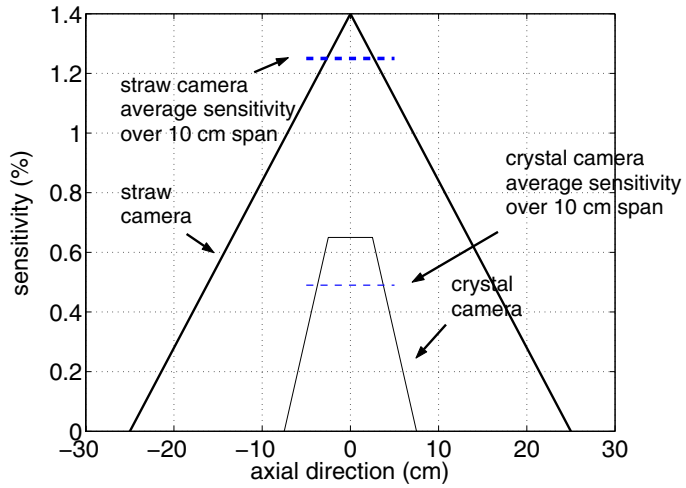

Fig. 2. Straw camera vs. crystal camera sensitivity. To achieve a reasonable axial field of view the crystal camera is operated in two axial positions centered at -2.5 cm and +2.5 cm, each taking up half of the total acquisition time. The maximum sensitivity is scaled to half of the fixed center-field sensitivity of 1.3%.

A. Methods

A pair of 50 cm detector modules were constructed using 4 mm diameter LWS and resistive 20 μm anode wire. Each module consisted of 50 straws in a 5 $\times$ 10 arrangement, attached on both ends to custom-designed end boards that allowed for gas flow, high voltage coupling, and anode wire tensioning. Straw decoding within a single module was accomplished by connecting groups of either rows or columns of straws together into delay line taps through terminating resistors and timing the delay line outputs to determine into which tap current was injected [1]. When a signal is produced in a straw, the current splits in inverse proportion to the distance from the end of the straw, producing a signal from each end (A and B). The longitudinal coordinate is obtained by taking the ratio of A/(A+B). This method is applied in the 50-straw module by digitizing the sum of the delay line output signals at each end of the module. Hence complete readout of a module is achieved with low-cost front-end electronics consisting of only two small PCBs (one on each end of the detector) connected to two ADCs and two TDCs. Intrinsic longitudinal spatial resolution of the detector module was measured using a slit-collimated ^{99}Tc source.

Coincidence imaging studies were performed in two different configurations as shown in Figures 3 and 4. In the first configuration two 50 cm long 50-straw modules were positioned parallel to one another as shown in Figure 3(a). To simulate detector pair rotation, phantoms were rotated continuously at 1 RPM about the Z-axis using a motor-driven turntable, and angle encoding was performed to a resolution of 0.1^o. Image reconstructions were done in the XY plane (Figure 3(b)). This configuration explores a possible geometry for breast cancer imaging and investigates the tradeoffs of image acquisition with and without detector rotation.

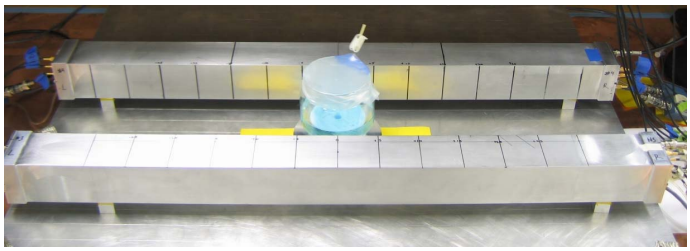

(a)

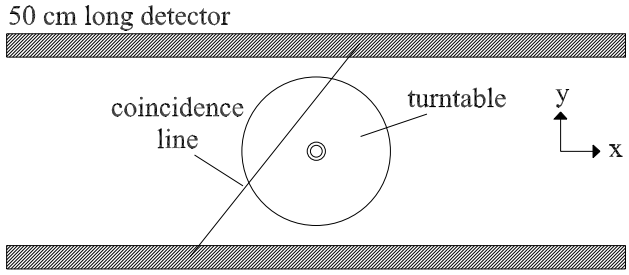

(b)

Fig. 3. Breast PET Configuration (a) Two 50-straw modules in their respective aluminum housings with a phantom placed between them. (b) Top view showing coordinate system, turntable equipped with angle encoder, and two 50-straw modules.

TABLE I
BREAST CONFIGURATION IMAGES

Phantom	Detector Separation	Image Plane	Rotation
82 μCi ^{22}Na point	15 cm	XY	Z-axis
Derenzo phantom	15 cm	XY	Z-axis
82 μCi ^{22}Na point	5 cm	XY	None

Table I lists the parameters for each image acquired in breast PET configuration. Rotation about the Z-axis was performed to simulate detector rotation in all cases except the 5 cm spaced case where use of the intrinsic wide angular acceptance in static mode was investigated. The Derenzo-like hole phantom was composed of three 5 mm, six 4 mm, ten 3 mm, and fifteen 2 mm holes. Adjacent holes were separated by a distance equal to four times the hole diameter. Simple FBP was used for image reconstruction. Sensitivity was measured as the ratio of the coincidence rate over the source activity.

TABLE II
SMALL ANIMAL CONFIGURATION IMAGES

Phantom	Detector Separation	Image Plane	Rotation
70 μCi ^{22}Na point	8 cm	YZ	X-axis
Hole phantom	8 cm	XY	X-axis

In the second configuration, a possible small animal imaging geometry, two 50 cm long 50-straw modules were positioned parallel to each other with a separation of 8 cm and were mounted in a rotating gantry as shown in Figure 4(a) providing 1 RPM detector rotation about the longitudinal X-axis (-90^o to 90^o). Using the coordinate system shown in Figure 4(b)), Table II lists the parameters for each image acquired. A grid of 1 cm spaced point sources was imaged in the XY plane by imaging a single ^{22}Na source at several positions with identical acquisition times. Point source reconstruction used simple FBP while MLEM was used to reconstruct the hole phantom.

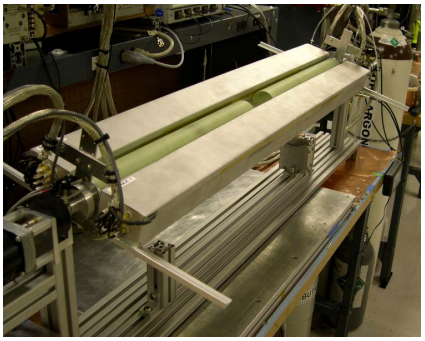

(a)

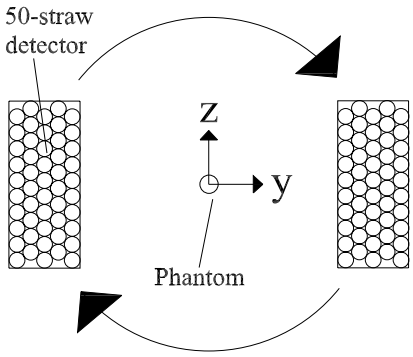

(b)

Fig. 4. Small Animal PET Configuration (a) Rotating small animal PET camera consisting of two 50 cm long, 50-straw detector modules and 8 cm bore diameter. (b) End view showing coordinate system definition.

II. Results

Figure 5 shows individual module resolution results produced by the finely-collimated ^{99}Tc source. The mean intrinsic spatial resolution of a typical 50-straw module was 3.3 mm FWHM.

In the breast PET configuration, at 15 cm detector separation, the point source produced a resolution of 4.3 mm FWHM (Figure 6(a)). At 5 cm detector separation with no rotation, the point source produced 4.3 mm $\times$ 3.3 mm FWHM (Figure 6(b)). Figure 7 shows the image produced by the Derenzo-like hole phantom. Coincidence count rate with 15 cm detector separation for the point source at CFOV was 550 cps resulting in a sensitivity of 0.018%.

In the small animal configuration, the ^{22}Na point source imaged in the YZ plane produced a resolution of 3.9 mm $\times$ 3.3 mm FWHM (Figure 8). The hole pattern imaged is shown in Figure 9 and has an average FWHM resolution per spot of 4.3 mm $\times$ 3.7 mm.

A plot of the sensitivity variation in both the X and Y directions is shown in Figure 10 illustrating the relatively constant sensitivity across the detector field of view. The center field sensitivity was 0.044%.

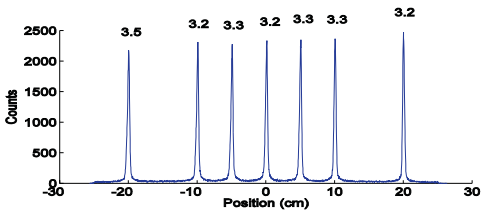

Fig. 5. Position spectra in the direction along the X-axis, using a collimated ^{99}Tc source. FWHM resolutions shown in mm.

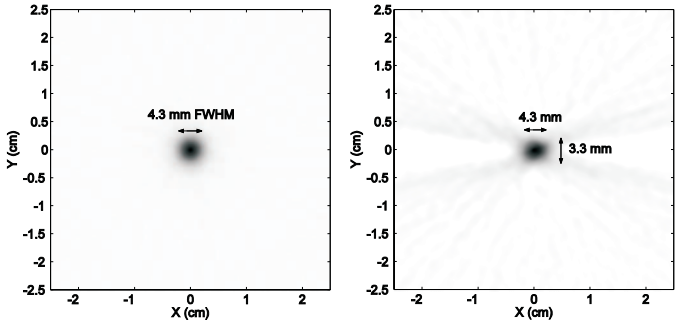

(a) (b)

Fig. 6. Image of point source in breast PET configuration (a) at 15 cm detector separation with rotation about the Z-axis (b) at 5 cm detector separation with no rotation.

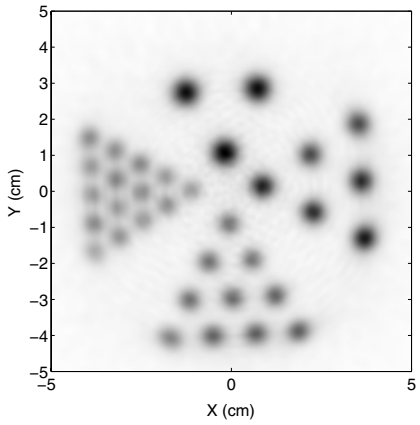

Fig. 7. Image of the Derenzo phantom in breast PET configuration.

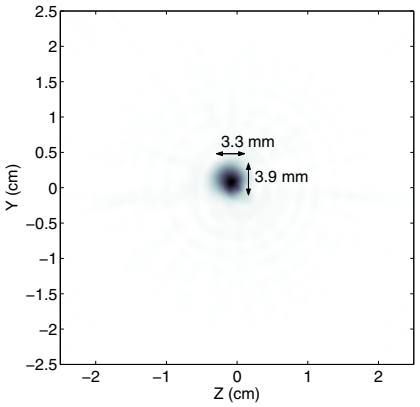

Fig. 8. Image of 70 μCi ^{22}Na point source acquired in small animal configuration and reconstructed in the YZ plane.

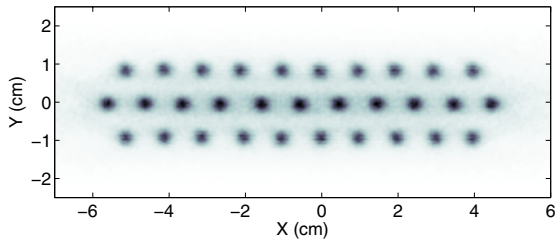

Fig. 9. Pattern composed of 1 cm spaced ^{22}Na point sources in small animal configuration with no uniformity correction. A large 11 cm field of view was achieved without detector repositioning.

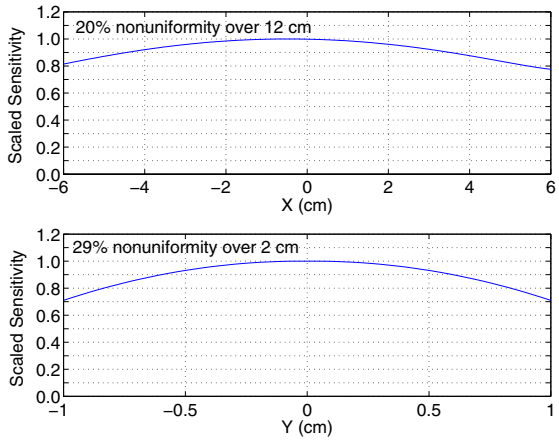

Fig. 10. Detector sensitivity in both the X and Y directions.

III. Summary & Discussion

In summary, testing of a pair of detector modules each composed of 50 50-cm long, 4 mm diameter lead wall straws shows promise in two specialized but very important PET applications.

In the breast imaging phantom studies simulating 5 cm compressed geometry (fixed no detector rotation), imaging resolution was found to be little affected by lack of rotation. Therefore, long linear LWS detectors can likely be used for breast imaging in a static mode as a result of the very large angular sampling afforded by the lengthy detectors. If required, the detectors can also be rotated to allow for larger detector separation without loss of angular coverage. In small animal imaging, the long detector lengths allow for very large field of views and high camera sensitivity without the need for many detector elements. The detectors are light and easily rotated to achieve the angular sampling required.

The precise 3D encoding capability and ease of construction into long lengths afforded by this technology provides large angular acceptance and rigorously parallax-free imaging with the option of rotation to achieve uniform angular acceptance if necessary. This new technology can also markedly reduce costs over crystal systems. Straws can be made arbitrarily long at very low cost with high speed winding techniques, and detector readout is performed very cheaply with a single amplifier board at each of the 50-straw detector module. As a result, LWS detectors are very attractive for use in low-cost high-performance specialized PET cameras.

Acknowledgment

Funding of this project was provided by NIH grant nos. RR13482 and RR15993. We would also like to thank Dan Kadrmas for performing the MLEM image reconstruction.

References

[1] A. Athanasiades, N. N. Shehad, C. S. Martin, L. Sun, and J. L. Lacy, "Straw Detector for High Rate, High Resolution Neutron Imaging," in *IEEE Nuclear Science Symposium Conference Record*, 23-29 Oct. 2005.